ACS APPLIED MATERIALS & INTERFACES

Research Article

www.acsami.org

Passivated Iodine Pentoxide Oxidizer for Potential Biocidal Nanoenergetic Applications

Jingyu Feng, Guoqiang Jian, Qing Liu, and Michael R. Zachariah*

Department of Chemistry and Biochemistry, and Department of Chemical and Biomolecular Engineering, University of Maryland, College Park, Maryland 20742, United States

Supporting Information

ABSTRACT: Iodine pentoxide (I_2O_5), also known as diiodine pentoxide, is a strong oxidizer which has been recently proposed as an iodine-rich oxidizer in nanoenergetic formulations, whose combustion products lead to molecular iodine as a biocidal agent. However, its highly hygroscopic nature hinders its performance as a strong oxidizer and an iodine releasing agent and prevents its implementation. In this work, we developed a gas phase assisted aerosol spray pyrolysis which enables creation of iron oxide passivated I_2O_5. Transmission electron microscopy elemental imaging as well as temperature-jump mass spectrometry confirmed the core shell nature of the material and the fact that I_2O_5 could be encapsulated in pure unhydrated form. Combustion performance finds an optimal coating thickness that enables combustion performance similar to a high performing CuO based thermite.

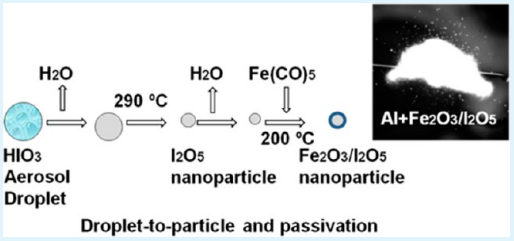

KEYWORDS: *passivated, aerosol spray pyrolysis, nanothermite, energetic materials, nanocomposite, biocide*

1. INTRODUCTION

Nanoenergetic materials, including metal based fuels and metal oxide oxidizers with typically nanosized dimensions, have been shown to have reactive properties superior to traditional energetic materials.[1−4] Essentially, our current understanding is that the importance of the nanoscale is to more intimately mix fuel and oxidizer, thus reducing the heat and mass transport limitations, leading to a significant enhancement in its reactivity and burn rate.[5−11]

The growing threat of biological weapons has prompted research efforts into new energetic materials with biocidal capabilities.[12−18] Such materials possess an energetic component to deliver thermal energy but also release biocidal agents, e.g., silver or halogen that can function over a longer period of time. For many applications, energetic components involve the use of aluminum as a fuel component with a strong oxidizer, which releases the biocide. Clark et al. showed from the group of energetic oxidizers, I_2O_5, Ag_2O, Fe_2O_3, that the iodine containing thermite was extremely effective at neutralizing spores postcombustion.[16] Other oxidizers including $AgIO_3$ and Ag_2O were investigated experimentally for potential biocidal applications.[17,18] $AgIO_3$, which thermally decomposed to release iodine and oxygen, was shown to have better performance than the traditional oxidizers copper oxide and iron oxide in nano-Al based combustion tests.[17] Ag_2O, a relatively poor oxidizer, if combined with CuO and $AgIO_3$, can generate a high amount of biocidal silver in nanoaluminum based thermite reactions.[18]

Due to the biocidal property of iodine, other oxidizers are being considered, most notably I_2O_5 which is a very strong oxidizer with a high mass fraction of iodine (~76%).[19] "Al + I_2O_5" reaction has been shown to be effective at neutralizing spores, presumably because of the release of elemental iodine as a combustion product when reacted with aluminum:[16] $10Al + 3I_2O_5 \rightarrow 5Al_2O_3 + 3I_2$. However, I_2O_5 is sensitive to humid environments and reacts with water in the ambient air.[20,21] This not only increases the particle size which degrades combustion performance but also hydrolyzes I_2O_5 to iodic acid HIO_3[20,21] which is corrosive to metal. HIO_3 will undergo reaction with elemental aluminum to give aluminum oxide under ambient conditions.[22] This not only severely limits the combustion performance of I_2O_5 containing thermite but also inhibits I_2O_5's application as an iodine-releasing oxidizer for agent defeat in thermite formulations. To address this limitation, one approach is to create the passivated structure for I_2O_5 particles.

Several methods that are currently available to fabricate passivated nanoparticles can be generally classified into two categories: "wet treatment"[23] and "gas phase".[24] The approaches involving "liquid phase", such as the co-precipitation, sol-gel, and microemulsion, dispersing core particles in a solvent containing reactive precursors, are not applicable to passivate I_2O_5.[20] The alternative "gas phase" methods, which have the possibility to scale up,[24] are easier and more suitable to make passivated I_2O_5 nanoparticles.

Prakash et al. reported a single step, two-temperature aerosol spray pyrolysis process to create a pure core−shell nanostructure for nanothermite formulations, whereby a thin layer of relatively weak oxidizer (Fe_2O_3) was coated on a strong oxidizer ($KMnO_4$) nanoparticle.[25] In this process, precursors of $Fe(NO_3)_3{\cdot}9H_2O$ and $KMnO_4$ are dissolved in an aqueous

Received: January 14, 2013
Accepted: August 29, 2013
Published: August 29, 2013

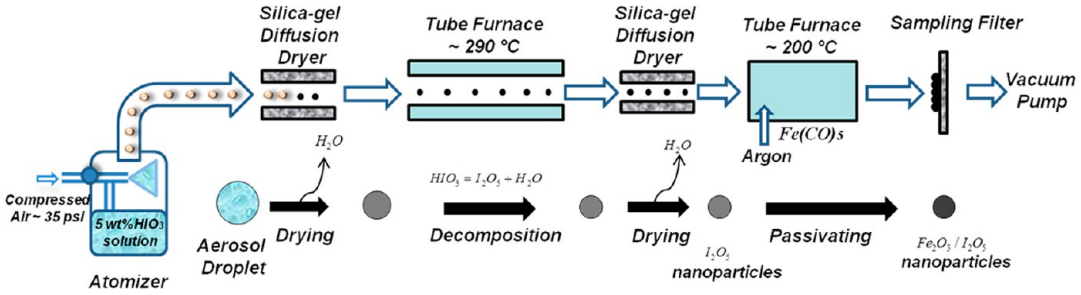

Figure 1. Experimental system for synthesis of I_2O_5 and its passivation with iron oxide.

solution and sprayed into droplets that are typically one micrometer in diameter. The droplets pass through the diffusion dryer and to two tube furnaces maintained at different temperatures. The first furnace was maintained above the iron nitrate decomposition temperature (~120 °C), and the second furnace was operated at the temperature near the melting point of potassium permanganate (~240 °C). At 120 °C, the iron nitrate decomposes into Fe_2O_3, in the permanganate solid matrix. When the temperature is raised to 240 °C, where the permanganate melts, Fe_2O_3 phase separates and aggregates as a shell around the $KMnO_4$ core. The reactivity of the resulting materials can be tuned by coating the $KMnO_4$ core with Fe_2O_3 shell of different thicknesses.[25] This approach can also be generalized and applied to other systems. For example, Wu et al. employed this strategy to successfully incorporate high oxygen content perchlorate salts ($KClO_4$ and NH_4ClO_4) into the common metal oxide (Fe_2O_3 and CuO) shell.[26] The key to this strategy is to take advantage of the aerosol spray pyrolysis method, where all the physical and chemical processes occur in the confined aerosol droplet as a micro-reactor.

Although the above-mentioned single step, two-temperature aerosol spray pyrolysis strategy is simple, it failed to passivate I_2O_5 particles because the shell precursors, $Fe(NO_3)_3$ and $Cu(NO_3)_2$, reacted immediately with iodic acid to form metal iodate precipitates in the starting solution. Thus, an alternative approach was required.

In this work, we developed a modified gas phase assisted aerosol synthesis approach to successfully passivate I_2O_5 within an iron oxide shell to create an air-stable passivated oxidizer. The size, morphology, and composition characterizations of the as prepared Fe_2O_3/I_2O_5 passivated oxidizer were done by a transmission electron microscope (TEM) with an energy dispersive X-ray spectrometer (EDS). A time resolved high heating rate mass spectrometer was employed to characterize the reactivity. These nanocomposite materials were then formulated into nanoaluminum based thermite mixtures to evaluate their reactive properties as an oxidizer. The final product shows a violent reaction when formulated with nanoaluminum, demonstrating a larger pressurization rate and transient peak pressure. The long term stability measurement results were evaluated by exposing the sample in ambient air and monitoring weight changes over a ten day period as detailed in the Supporting Information. Over this period, the material was increased by no more than +1.6% indicating that the passivated oxidizers have good long term stability when exposed to ambient air.

2. EXPERIMENTAL SECTION

2.1. Materials. Iodic acid (HIO_3, 99.5%), iodine pentoxide powder (I_2O_5, 99.99%), iron pentacarbonyl ($Fe(CO)_5$, >99.99%), reference Fe_2O_3 nanopowder (<50 nm), and CuO nanopowder (< 50 nm) were from Sigma-Aldrich and used as received. The nano-sized aluminum (~50 nm ALEX) for the thermite reaction was purchased from the Argonide Corporation. The aluminum nanopowders were measured to contain 70 wt % active Al by thermogravimetric analysis (TGA).

2.2. Aerosol Spray Pyrolysis and Materials Characterization. Aerosol spray pyrolysis includes two steps: atomization and thermal decomposition (Figure 1). In the atomization step, the dissolved precursor solution was atomized to produce the aerosol droplets by a home-made Collison-type atomizer. The droplet diameter was measured to be around 1 μm by a laser aerosol spectrometer. Aerosol droplets were firstly passed through a diffusion dryer filled with silica gel to remove most of the precursor solvent (water) and then through tube furnaces for the thermal decomposition. In the atomizer, the precursor iodic acid solution concentration was 5.0 wt %. The residence time of the reaction was estimated to be ~8 seconds at a flow rate of 3.5 L/min. The final iron oxide coated I_2O_5 products were collected on a HTTP membrane filter (0.4 μm pore, Millipore). TEM (JEOL JEM 2100 FEG) and EDS (Oxford INCA 250) line scans provided information of particle size, morphology, and elemental core−shell structure.

2.3. Iron Oxide Passivation Coating. Iron oxide was chosen as a passivating coating because of its prior success in passivating potassium permanganate.[25] The iron oxide coating was fabricated via a thermal decomposition method, in which iron pentacarbonyl is vaporized and decomposed followed by deposition onto the surface of the I_2O_5. Iron pentacarbonyl vapor was generated by introducing a metered flow of argon into the liquid in an ice bath. The vapor was then mixed with the aerosol stream and decomposed at ~200 °C.

Assuming all the iron pentacarbonyl decomposed and ended up as iron oxide on the surface of I_2O_5 core particles, the coating thickness, for volumetric flow rates of argon at 26, 75, 210, and 300 sccm, is calculated to be 4.3, 12, 34, and 49 nm. The related Fe/I molar ratios were determined gravimetrically (detailed in 2.4.1.) to be 0.25, 1.8, 4.3, and 6.2, respectively.

2.4. Combustion Tests. *2.4.1. Thermite Sample Preparation.* In order to create a stoichiometric thermite mixture with nanoaluminum, knowledge of the ratio of iron to iodine in the oxidizer is needed. The reaction chemistry for the thermite combustion reaction is:

$$(6a + 10)\mathrm{Al} + 3[a\mathrm{Fe_2O_3} + \mathrm{I_2O_5}] \rightarrow (3a + 5)\mathrm{Al_2O_3} + 6a\mathrm{Fe} + 3\mathrm{I_2}$$

$[a\mathrm{Fe_2O_3} + \mathrm{I_2O_5}]$ is the passivated I_2O_5 with the Fe/I molar ratio a which was determined by a measurement of the oxidizer's weight loss during the thermal decomposition of I_2O_5 at a temperature of 600 °C,[27] the remaining weight being only the iron oxide, using a Sartorius SE2 Ultra Micro Balance (Sartorius AG). The appropriate amounts of nanoaluminum fuel and oxidizer were weighed out and mixed in hexane and then sonicated for 30 min. The as prepared mixture was kept in the fume hood overnight to allow for the evaporation of the hexane (or in a vacuum dryer at room temperature for 3 or 4 h). The dry powder was gently broken apart to obtain a loose powder before the test.

2.4.2. Combustion Cell Evaluation. To evaluate performance, simultaneous pressure and optical measurements were conducted in a

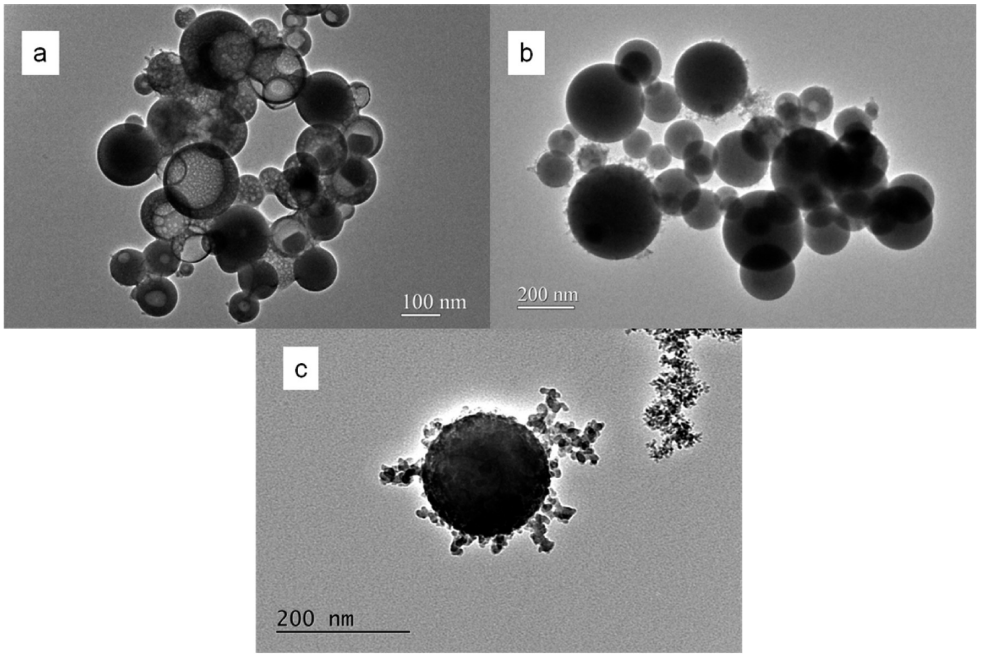

Figure 2. TEM image of Fe_2O_3/I_2O_5 passivated oxidizer with a Fe/I molar ratio of (a) 0.25; (b) 1.8; (c) 4.3.

constant-volume combustion cell[26,28,30] to characterize the reactivity of the prepared thermite samples. Since the measurement of the thermite reactivity is a relative experiment, both the pressure and optical emission tests are reported along with reference oxidizers: Fe_2O_3 and CuO nanoparticles. In a typical combustion cell experiment, a thermite sample powder (25 mg), with the correct stoichiometry, was loaded in a combustion cell (constant volume, ~13 cm^3) and ignited by resistive heating with a nichrome wire. After ignition, the data collection was triggered by the rising optical signal. A fast time response piezoelectric pressure transducer was employed to measure the transient pressure pulse. The optical emission in the combustion event was simultaneously collected by a lens tube and recorded by an optical detector. Both the pressure and optical signals were recorded by an oscilloscope. The pressurization rate is expressed as the peak pressure (KPa) divided by the pressure rise time (μs). The characteristic burn time of thermite in the combustion cell is arbitrarily represented by the full width at half-maximum (FWHM) of the recorded optical signal intensity. The details of the combustion cell test can be found in our prior publications.[26,28,29]

2.4.3. Temperature-Jump/Time-of-Flight Mass Spectrometry (T-Jump/TOFMS). To evaluate the decomposition behavior of the passivated I_2O_5, a rapid heating experiment coupled to mass spectrometry was employed. In these experiments, a thin layer of passivated I_2O_5 sample (Fe/I molar ratio: 4.3) was coated onto a ~12 mm long platinum wire (diameter: ~76 μm) which was rapidly resistively heated to ~1800 K in 3 ms at a heating rate of $\sim 5 \times 10^5$ K/s. The temporal measured wire resistances are used to determine the temporal filament temperature. More detailed information of the T-Jump mass spectrometry can be found in our previous publications.[30,31]

2.4.4. High-Speed Imaging. High speed imaging of the wire tests was conducted under atmospheric conditions using a high-speed digital camera (Phantom v12.0, Vision Research). The high speed video (256 × 256 resolution) was recorded at the frame rate of 67 065 fps (14.9 μs per frame).

3. RESULTS AND DISCUSSION

3.1. Synthesis of Passivated I_2O_5. The basic idea of this aerosol coating approach is to first synthesize aerosol particles of I_2O_5, which can then be passivated in situ with a layer of iron oxide using controlled thermal decomposition of iron pentacarbonyl in air. The objective is to use the I_2O_5 nanoparticles as the substrate for the iron oxide to deposit onto, thus allowing them to form a core−shell passivated structure.

The experimental setup is schematically depicted in Figure 1. As shown in Figure 1, I_2O_5 particles were produced using aerosol spray pyrolysis with air as the carrier gas in the first furnace heated to ~290 °C, which is above the reported decomposition temperature (~207 °C) for $2HIO_3 = I_2O_5 + H_2O$ and below the reported decomposition temperature of I_2O_5 (~391 °C)[27] Thus, starting with aqueous solutions of HIO_3, the sprayed aerosol droplets from the atomizer were delivered through a diffusion dryer to remove most of water in the droplets. The first furnace at 290 °C should fully decompose iodic acid to iodine pentoxide and water. A second diffusion dryer was introduced to absorb the water produced during the iodic acid decomposition, to ensure that particles entering the second furnace were I_2O_5 and did not revert back to iodic acid.

To create the coated I_2O_5 particles, the iron pentacarbonyl precursor vapor was introduced downstream of the I_2O_5 particles at ~200 °C where the iron pentacarbonyl decomposed to iron and carbon monoxide.[32] The delivery rate of the iron pentacarbonyl into the second furnace is controlled by the flow rate of the argon while the flow rate of I_2O_5 particles is kept constant.

3.2. Characterizations of the Passivated I_2O_5 (Size, Structure, Morphology, and Composition). The synthesized particles were characterized by several techniques including TEM, elemental analysis, and time resolved mass spectrometry. The $Fe(CO)_5$ was introduced into the second furnace with the argon flow rate at 26, 75, and 210 sccm. The related Fe/I molar ratios were determined, using the weighing measurement, to be 0.25, 1.8, and 4.3, respectively. The particles were further examined by TEM with EDS line scans. Figure 2a shows the representative TEM image of the final product with a Fe/I molar ratio of 0.25 obtained at the argon flow rate of 26 sccm. At these low concentrations, we observed

dx.doi.org/10.1021/am4028263 | ACS Appl. Mater. Interfaces 2013, 5, 8875−8880

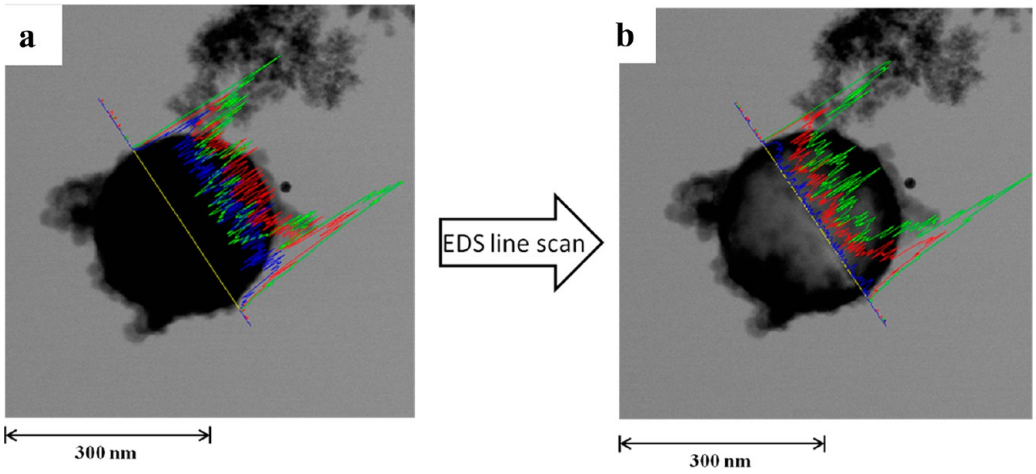

Figure 3. Typical TEM image of Fe_2O_3/I_2O_5 passivated oxidizer product (Fe/I molar ratio: 4.3) with elemental line scan (green: iron; red: oxygen; blue: iodine): (a) EDS line scan profile of a solid particle. (b) EDS line scan elemental profile of a hollow particle obtained from (a) after an EDS line scan.

only the spherical smooth shell passivated particles with no evidence of homogeneous nucleated fine particles of iron oxide. The TEM images show the particles in some cases have a hollow like structure, resulting from heating by the electron beam of the microscope, which indicates an incomplete coating. In fact, one can see in some cases iodine containing crystals in some hollow structured particles. Figure 2b shows a TEM image of Fe_2O_3/I_2O_5 passivated oxidizer with a Fe/I molar ratio of 1.8. The particles have a mean diameter of ca. 200 nm. Closer scrutinization reveals a clear fractal structure that extends from the surface of particles, implying that some gas phase homogeneous nucleation of the iron oxide was taking place.

At a higher concentration of iron pentacarbonyl, corresponding to a Fe/I molar ratio of 4.3, the final product shows evidence of considerable homogeneous nucleation of the iron (which will subsequently be converted to iron oxide outside the reactor). Figure 2c shows an Fe_2O_3/I_2O_5 passivated oxidizer particle, with a large fraction of fractal aggregates on the I_2O_5 particles' surface. Figure 3 shows the TEM image of passivated oxidizer product (Fe/I molar ratio: 4.3) with an elemental line scan. As shown in Figure 3a, the obtained core/shell type particle has an iodine oxide core and an iron oxide shell. A cleared view of the core−shell material of the particle is seen in Figure 3b, whose image is taken after the elemental scan, which apparently caused sufficient heating to decompose the I_2O_5 and evaporate the I_2, revealing the remaining iron-oxide shell. The shell thickness appears to be close to ∼34 nm which was estimated assuming all the iron pentacarbonyl decomposed and ended up as iron oxide on the surface of I_2O_5 core particles.

T-Jump/TOFMS was employed to characterize the species formed during rapid heating, which might be encountered in a combustion event. For these experiments, the passivated oxidizers were rapidly heated on a fine wire to ∼1800 K in 3 ms, and a time resolved MS of the species produced in the reaction was obtained. Figure 4 shows the time resolved MS of the Fe_2O_3/I_2O_5 nanocomposite oxidizer under a heating rate of $\sim 5 \times 10^5$ K·s^{-1}. O_2, I, and I_2 are the primary species produced commencing at ∼920 K (t = 1.4 ms). The H_2O peak is attributed to the background species in the mass spectrometer. Note that only I, I_2 without any other iodine suboxides species, is observed, suggesting that the I_2O_5 is successfully encapsulated by iron oxide, which prevents the I_2O_5 from forming iodic acid when exposed to humidity in the ambient air.[33]

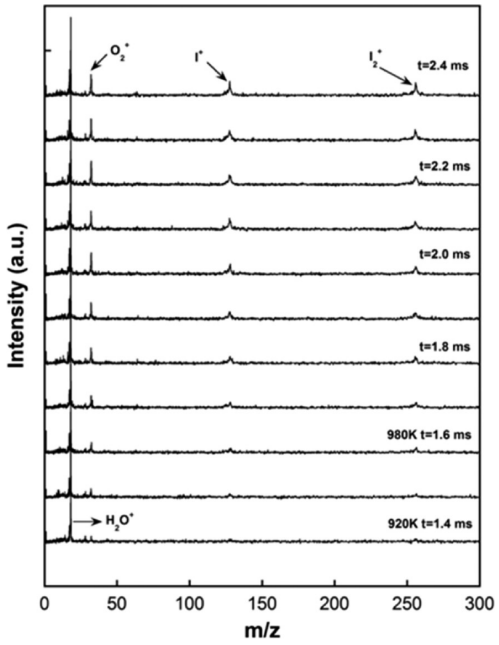

Figure 4. Time resolved mass spectra of the Fe_2O_3/I_2O_5 passivated oxidizer with a Fe/I ratio of 4.3 under rapid heating. Note: heating pulse is ∼3 ms, i.e., heating rate of $\sim 5 \times 10^5$ K·s^{-1}.

3.3. Combustion Characterization of "nano-Al + (Fe_2O_3/I_2O_5)" Thermite System. High-speed digital photography to observe the reactive behavior was carried out at a high heating rate of∼ 5×10^5 K·s^{-1} on a platinum wire (76 μm diameter), for which selected snapshots are shown in Figure 5. The iodine pentoxide-containing thermite system clearly shows a violent reaction over a period of ∼2000 μs.

The relative combustion performance of "Al + (Fe_2O_3/I_2O_5)" thermite against the reference thermite "Al + nano-Fe_2O_3" and "Al + nano-CuO" was evaluated in a combustion cell (constant volume). Table 1 summarizes the experimental results of pressure and optical emission for thermite samples prepared with different oxidizers. Clearly, the "Al + (Fe_2O_3/I_2O_5)" thermite with Fe/I molar ratio of 1.8 and 4.3

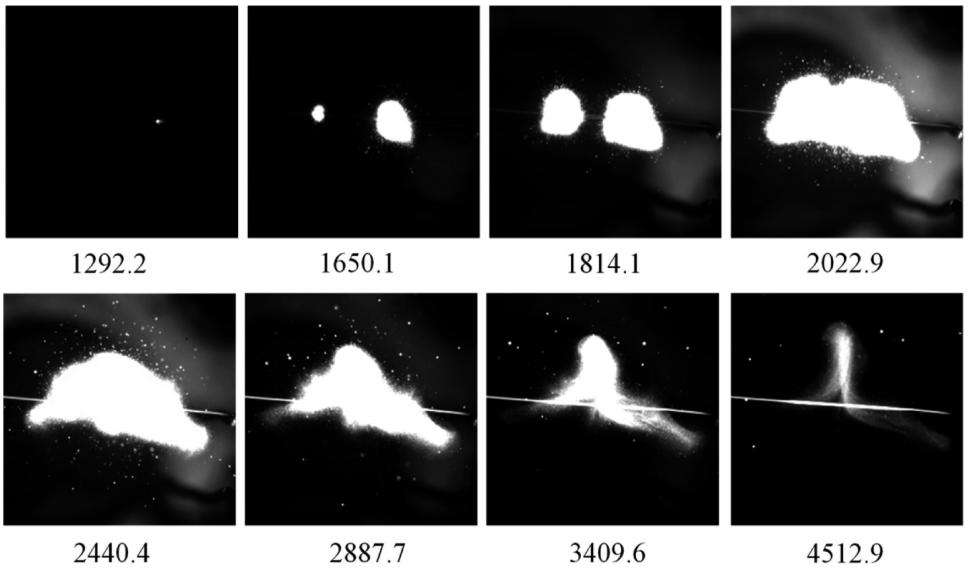

Figure 5. Selected sequential snapshots of "nano-Al + (Fe_2O_3/I_2O_5)" burning on rapid-heating platinum wire in air recorded by a high speed camera. The numbers below the images are time elapsed (μs) after heating triggered (T = 883 K at 1292.2 μs). The thermite is nano-Al (ALEX) and nanocomposite oxidizer Fe_2O_3/I_2O_5 with a Fe/I molar ratio of 4.3.

Table 1. Combustion Cell Test Data for Thermite Samples Prepared with Different Oxidizers[a]

oxidizers (w/nanoaluminum, φ = 1)	molar ratio of Fe/I	P_{rise} (KPa)	pressure rise time (μs)	pressurization rate (KPa/μs)	FWHM burn time (μs)	note
Fe_2O_3/I_2O_5	0.25	152	1530	0.0896	1910	aerosol + iron pentacarbonyl
	1.8	1262	28	45.1	183	
	4.3	821	24	35.2	119	
	6.2	108	2970	0.0363	4280	
nano-Fe_2O_3 (ref.)	N/A	92.4	800	0.116	936	<50 nm, Sigma-Aldrich
nano-CuO (ref.)	N/A	800	13	61.5	192	

[a]All six oxidizers were physically mixed with aluminum nanopowder (ALEX). Thermite sample was prepared with a specific stoichiometry assuming complete conversion of Al to Al_2O_3. Note: The reported pressurization rate has an uncertainty of <10% based on two runs.

outperforms "Al + nano-Fe_2O_3" in both pressurization rate and transient peak pressure and with shorter FHWM burning time. However, the formulated nanothermite does not exceed the performance of "Al + nano-CuO", when directed comparing their pressurization rates, as shown in Figure 6.

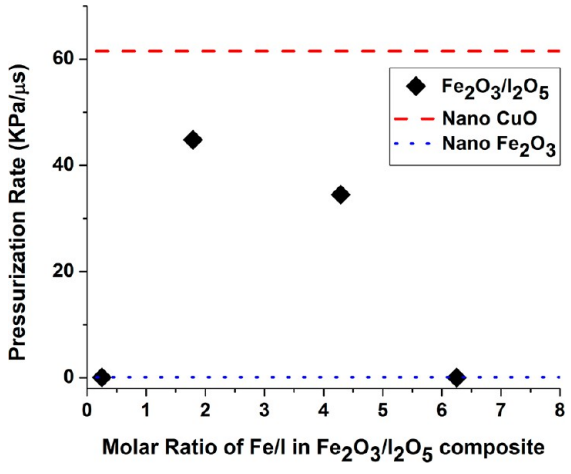

Figure 6. Pressurization rate for thermite samples prepared with Fe_2O_3/I_2O_5 with different Fe/I molar ratios in the composite particles. The nano-CuO and nano-Fe_2O_3 were used here as reference oxidizers.

In our previous study, we have argued that the pressurization happens as a result of releasing oxygen from the decomposition of oxidizer, which occurs well before significant optical emission.[26,29] A nanothermite system like Al/CuO nanothermite has a rapid pressure rise followed by an optical signal due to the rapid oxygen release of CuO.[8,26] This is consistent with Table 1, which illustrates that the time scale of optical emission of "Al + nano-CuO" is larger than that of the pressure rise time. Unlike "Al + CuO", the pressure and optical signals of "Al + Fe_2O_3" occur almost concurrently in which the decomposition of Fe_2O_3 becomes the rate-limiting step.[26,29]

In addition, we might moderate the thickness of the shell by varying the ratio of iron to iodine and evaluate the effect of shell thickness on combustion performance. The oxidizers with Fe/I molar ratio of 0.25 and 6.2 in Table 1 show similar relative behavior as an "Al + Fe_2O_3" thermite, i.e., a nanothermite with poor performance: the pressure rise times are similar to the time scales of the optical emission, which indicates the pressure signal and the optical emission occurred almost concurrently. At low Fe/I molar ratios (0.25), the poor performance can be attributed to insufficient surface coverage to fully passivate I_2O_5. At the other extreme, a large excess of iron (Fe/I = 6.2) also serves to degrade performance, with reactive behavior even poorer than pure iron oxide. When the Fe/I molar ratio is 1.8 or 4.3, the thermites show a similar relative behavior as Al/CuO nanothermite, a rapid rising pressure signal followed by a prolonged optical emission (the pressure rise times are much

dx.doi.org/10.1021/am4028263 | ACS Appl. Mater. Interfaces 2013, 5, 8875−8880

shorter than FHWM burn times), as shown in Table 1, indicating that the I_2O_5 nanoparticles are well passivated by Fe_2O_3 and have a similar burning mechanism as CuO. Thus, the reactivity of Fe_2O_3/I_2O_5 passivated oxidizer can be tuned by varying the Fe/I ratio.

4. CONCLUSION

In summary, hygroscopic strong oxidizer I_2O_5 was successfully passivated into Fe_2O_3 metal oxide shell through a modified gas phase assisted aerosol approach. We find that reactivity can be tuned by varying the Fe/I molar ratio using a controlled thermal decomposition of iron pentacarbonyl. TEM with EDS line scan shows that the nanocomposite is composed of core/shell Fe_2O_3/I_2O_5 nanoparticles with iron oxide nanoparticles. Mass spectroscopy indicates release of a significant amount of oxygen and iodine species (I and I_2) confirming pure I_2O_5 within the composite. The synthesized Fe_2O_3/I_2O_5 nanocomposites were formulated into nanoaluminum based thermite as an oxidizer, and its reactivity was evaluated by the combustion cell and rapid heating wire ignition test with simultaneous high speed imaging. Combustion tests reveal an optimal coating thickness that enables combustion performance similar to a high performing CuO based thermite.

■ ASSOCIATED CONTENT

Supporting Information

The long term stability experiment about the passivated oxidizer. This material is available free of charge via the Internet at http://pubs.acs.org.

■ AUTHOR INFORMATION

Corresponding Author

*E-mail: mrz@umd.edu. Phone: 301-405-4311. Fax: 301-314-947.

Notes

The authors declare no competing financial interest.

■ ACKNOWLEDGMENTS

Support for this work comes from the Defense Threat Reduction Agency. We acknowledge the support of the Maryland NanoCenter and its NispLab. The NispLab is supported in part by the NSF as a MRSEC Shared Experimental Facility.

■ REFERENCES

(1) Dreizin, E. L. *Prog. Energy Combust. Sci.* **2009**, *35*, 141−167.
(2) Piercey, D.G.; Klapötke, T. M. *Cent. Eur. J. Energ. Mater.* **2010**, *7*, 115−129.
(3) Yetter, R.A.; Risha, G.A.; Son, S.F. *Proc. Combust. Inst.* **2009**, *32*, 1819−1838.
(4) Jian, G.; Chowdhury, S.; Sullivan, K.; Zachariah, M.R. *Combust. Flame* **2013**, *160*, 432−437.
(5) Rossi, C.; Zhang, K.; Estève, D.; Alphonse, P.; Thailhades, P.; Vahlas, C. *J. Microelectromech. Syst.* **2007**, *16*, 919−931.
(6) Rossi, C.; Estève, A.; Vashishta, P. *J. Phys. Chem. Solids* **2010**, *71*, 57−58.
(7) Kim, S.H.; Zachariah, M.R. *Adv. Mater.* **2004**, *16*, 1821−1825.
(8) Jian, G.; Liu, L.; Zachariah, M. R. *Adv. Funct. Mater.* **2013**, *23*, 1341−1346.
(9) Malchi, J. Y.; Foley, T. J.; Yetter, R. A. *ACS Appl. Mater. Interfaces* **2009**, *1*, 2420−2423.
(10) Yan, S.; Jian, G.; Zachariah, M.R. *ACS Appl. Mater. Interfaces* **2012**, *4*, 6432−6435.
(11) Séverac, F.; Alphonse, P.; Estève, A.; Bancaud, A.; Rossi, C. *Adv. Funct. Mater.* **2012**, *22*, 323−329.
(12) Zhang, S.; Badiola, C.; Schoenitz, M.; Dreizin, E.L. *Combust. Flame* **2012**, *159*, 1980−1986.
(13) Zhang, S.; Schoenitz, M.; Dreizin, E.L. *J. Phys. Chem. C* **2010**, *114*, 19653−19659.
(14) Grinshpun, S.A.; Adhikari, A.; Yermakov, M.; Reponen, T.; Dreizin, E.; Schoenitz, M.; Hoffmann, V.; Zhang, S. *Environ. Sci. Technol.* **2012**, *46*, 7334−7341.
(15) Fischer, D.; Klapötke, T.; Stierstorfer, J. *Z. Anorg. Allg. Chem.* **2011**, *637*, 660−665.
(16) Clark, B. R.; Pantoya, M. L. *Phys. Chem. Chem. Phys.* **2010**, *12*, 12653−12657.
(17) Sullivan, K.; Piekiel, N.; Chowdhury, S.; Wu, C.; Johnson, C.; Zachariah, M. R. *Combust. Sci. Technol.* **2011**, *183*, 285−302.
(18) Sullivan, K.; Wu, C.; Piekiel, N.; Gaskell, K.; Zachariah, M. R. *Combust. Flame* **2013**, *160*, 438−446.
(19) Martirosyan, K. S. *J. Mater. Chem.* **2011**, *21*, 9400−9405.
(20) Wiberg, E.; Wiberg, N.; Holleman, A. F. *Inorganic Chemistry*, 1st ed.; Academic Press: New York, 2001; p 465.
(21) Earnshaw, A.; Greenwood, N. *Chemistry of Elements*, 2nd ed.; Butterworth-Heinemann: Oxford, 1997; p 852.
(22) Johnson, C. E.; Higa, K.T. *MRS Proc.* **2013**, 1521.
(23) Chaudhuri, R. G.; Paria, S. *Chem. Rev.* **2012**, *112*, 2373−2433.
(24) Zhang, L.; Ranadeb, M. B.; Gentry, J. W. *J. Aerosol Sci.* **2004**, *35*, 457−471.
(25) Prakash, A.; McCormick, A. V.; Zachariah, M. R. *Nano Lett.* **2005**, *5*, 1357−1360.
(26) Wu, C.; Sullivan, K.; Chowdhury, S.; Jian, G.; Zhou, L.; Zachariah, M. R. *Adv. Funct. Mater.* **2012**, *22*, 78−85.
(27) Farley, C.; Pantoya, M. *J. Therm. Anal. Calorim.* **2010**, *102*, 609−613.
(28) Prakash, A.; McCormick, A.; Zachariah, M.R. *Adv. Mater.* **2005**, *17*, 900−903.
(29) Sullivan, K.; Zachariah, M. R. *J. Propul. Power* **2010**, *26*, 467−472.
(30) Zhou, L.; Piekiel, N.; Chowdhury, S.; Zachariah, M. R. *Rapid Commun. Mass Spectrom.* **2009**, *23*, 194−202.
(31) Jian, G.; Piekiel, N.W.; Zachariah, M.R. *J. Phys. Chem. C* **2012**, *116*, 26881−26887.
(32) Giesen, A.; Herzler, J.; Roth, P. *J. Phys. Chem. A* **2003**, *107*, 5202−5207.
(33) Jian, G.; Chowdhury, S.; Feng, J.; Zachariah, M. R. In *8th U. S. National Combustion Meeting*, Park City, Utah, United States, May 19−22, 2013.